



Research article

Investigation of soliton solutions to the truncated M-fractional (3+1)-dimensional Gross-Pitaevskii equation with periodic potential

Haitham Qawaqneh¹, Ali Altalbe^{2,3}, Ahmet Bekir^{4,*} and Kalim U. Tariq⁵

¹ Department of Mathematics, Faculty of Science and Information Technology, Al-Zaytoonah University of Jordan, Amman 11733, Jordan

² Department of Computer Science, Prince Sattam Bin Abdulaziz University, Al-Kharj, Saudi Arabia

³ Faculty of Computing and Information Technology, King Abdulaziz University, Saudi Arabia

⁴ Neighbourhood of Akcaglan, Imarli Street, Number: 28/4, 26030, Eskisehir-Turkey

⁵ Department of Mathematics, Mirpur University of Science and Technology, Mirpur, Pakistan

* **Correspondence:** Email: bekirahmet@gmail.com; Tel: +905553689295.

Abstract: This research explores some modernistic soliton solutions to the (3+1)-dimensional periodic potential the Gross–Pitaevskii equation with a truncated M-fractional derivative plays a significant role in Bose–Einstein condensation, which describes the dynamics of the condensate wave function. The obtained results include trigonometric, hyperbolic trigonometric and exponential function solutions. Three techniques named: the \exp_a function method, the Sardar sub-equation method, and the extended (G'/G) -expansion approach are employed to achieve a variety of new solutions for the governing model. More comprehensive information about the dynamical representation of some of the solutions is being presented by visualizing the 2D, 3D and contour plots. This work reveals a number of new types of traveling-wave solutions, such as the double periodic singular, the periodic singular, the dark singular, the dark kink singular, the periodic solitary singular, and the singular soliton solutions. These novel solutions are not the same as those that were previously studied for this governing equation. The presented techniques demonstrate clarity, efficacy, and simplicity, revealing their relevance to diverse sets of dynamic and static nonlinear equations pertaining to evolutionary events in computational physics, in addition to other real-world applications and a wide range of study fields for addressing a variety of other nonlinear fractional models that hold significance in the fields of applied science and engineering.

Keywords: Gross–Pitaevskii equation; \exp_a function approach; Sardar sub-equation approach; extended (G'/G) -expansion approach; soliton solutions; fractional calculus

Mathematics Subject Classification: 35C07, 35Q51, 83C15

1. Introduction

Nonlinear evolution equations (NLEEs) have a wide range of applications in a variety of fields, including ocean engineering, solitary wave theory, hydrodynamics, optical fibers, chaos theory, and turbulence theory. The search for accessible qualities and the construction of exact solutions for nonlinear dynamical models are recognized to be critical to many nonlinear mathematical and physical processes. Many mathematical models have been developed in these areas in the form of nonlinear partial differential equations (NLPDEs). In literature, numerous schemes are developed to analyse such models like the generalized exponential rational function scheme [1], the Liu's extended trial function method [2], the generalized unified method [3], the $\exp(-\phi(\xi))$ approach [4], the sine-Gordon expansion technique [5], the enhanced modified simple equation scheme [6], the unified technique [7], the extended tanh function scheme [8], the Lie symmetry technique [9], the symbolic computational method, the Hirota bilinear approach [10], the long wave technique [11], the Jacobi elliptic function expansion scheme [12], the Elzaki transform decomposition technique [13], the $(m + \frac{1}{G})$ -expansion and adomian decomposition schemes [14], the extended modified auxiliary equation mapping technique [15], the simplest equation and Kudryashov's new function techniques [16], the modified simple equation scheme [17], the modified Kudryashov simple equation technique [18], the first integral technique [19], the Bäcklund transformation scheme [20], the extended jacobi elliptic function expansion technique [21], the extended (G/G) -expansion and the improved (G'/G) -expansion schemes [22], the Riemann-Hilbert approach [23], the modified Sardar sub-equation method [24], the polynomial expansion technique [25] and many others [26–33].

There are more convenient ways in the literature, such as the \exp_a function, the Sardar sub-equation and the extended (G'/G) -expansion methods, which have many prominent applications in contemporary research. For instance, some new analytical results of the perturbed Gerdjikov-Ivanov model have been achieved by using the \exp_a function and extended tanh function expansion methods in [34]. By applying the \exp_a function and hyperbolic function techniques, various kinds of wave solitons for a set of nonlinear Schrödinger equations are obtained [35]. Later on, different types of exact solitons of fractional (4+1)-dimensional Fokas equation are developed by utilizing the Sardar sub-equation method in [36]. Various kinds of wave solutions to the time-fractional parabolic equations have been obtained by applying the extended (G'/G) -expansion scheme [37, 38]. Currently, fractional calculus has gained much importance due to its various applications in different fields of scientific research.

Therefore, different definitions of fractional order derivatives have been introduced, like the conformable fractional derivative [39, 40], the beta derivative [41], the Caputo-Fabrizio fractional derivative [42], the truncated M-fractional derivative [43, 44] and many others. In this study, the truncated M-fractional (3+1)-dimensional Gross-Pitaevskii equation with periodic potential has been investigated analytically. In literature, Various approaches have been applied to construct different exact wave solutions for the governing model. For example, some new kinds of solitary wave solutions have been obtained by utilizing the Kudryashov method [45]. By applying the variational method, bright soliton solutions have been obtained in [46]. A collection of chirped-type exact wave solutions has been achieved by using the F-expansion technique [47].

The basic focus of this work is to investigate the truncated M-fractional (3+1)-dimensional Gross-Pitaevskii equation by employing the \exp_a function approach, the Sardar sub-equation approach, and

the extended (G'/G) -expansion approach. This study has different sections: Section 2: truncated M-fractional derivative and its characteristics; Section 3: model description; Section 4: description of methodologies; Section 5: mathematical treatment of model; Section 6: exact solutions of model; Section 7: conclusion.

2. Truncated M-derivative

2.1. Definition

Suppose $u(t) : [0, \infty) \rightarrow \mathbb{R}$, then the truncated M-derivative of u of order ϵ is given [48]

$$D_{M,t}^{\epsilon,\varrho} u(t) = \lim_{\tau \rightarrow 0} \frac{u(t E_{\varrho}(\tau t^{1-\epsilon})) - u(t)}{\tau}, \quad 0 < \epsilon < 1, \quad \varrho > 0, \quad (2.1)$$

where $E_{\varrho}(.)$ shows the truncated Mittag–Leffler function of one parameter that is defined as [49]

$$E_{\varrho}(z) = \sum_{j=0}^i \frac{z^j}{\Gamma(\varrho j + 1)}, \quad \varrho > 0 \text{ and } z \in \mathbf{C}. \quad (2.2)$$

2.2. Characteristics

Let $\epsilon \in (0, 1], \varrho > 0, r, s \in \mathbb{R}$, and g, f are ϵ -differentiable at a point $t > 0$, then by [48]:

$$(i) D_{M,t}^{\epsilon,\varrho}(rg(t) + sf(t)) = rD_{M,t}^{\epsilon,\varrho}g(t) + sD_{M,t}^{\epsilon,\varrho}f(t). \quad (2.3)$$

$$(ii) D_{M,t}^{\epsilon,\varrho}(g(t).f(t)) = g(t)D_{M,t}^{\epsilon,\varrho}f(t) + f(t)D_{M,t}^{\epsilon,\varrho}g(t). \quad (2.4)$$

$$(iii) D_{M,t}^{\epsilon,\varrho}\left(\frac{g(t)}{f(t)}\right) = \frac{f(t)D_{M,t}^{\epsilon,\varrho}g(t) - g(t)D_{M,t}^{\epsilon,\varrho}f(t)}{(f(t))^2}. \quad (2.5)$$

$$(iv) D_{M,t}^{\epsilon,\varrho}(A) = 0, \quad \text{where } A \text{ is a constant.} \quad (2.6)$$

$$(v) D_{M,t}^{\epsilon,\varrho}g(t) = \frac{t^{1-\epsilon}}{\Gamma(\varrho + 1)} \frac{dg(t)}{dt}. \quad (2.7)$$

3. The governing model

Consider the following (3+1)-dimensional Gross–Pitaevskii equation with a truncated M-fractional derivative [45]

$$\iota D_{M,t}^{\gamma,\varrho}g + \nabla g - U(x)g - \theta|g|^2g = 0, \quad (3.1)$$

where $g = g(x, y, z, t)$ represents a wave function, $|g|$ denotes a modulus value of g , while ∇ is a Laplacian operator, the nonlinear coefficient $\theta(x, y, z, t)$ represents a real-valued function that depends on the time and spatial coordinates, and the function $U(x)$ shows the periodic potential of the trap to confine the condensate. Eq (3.1) describes the Bose–Einstein condensate in the low temperature regime. This equation appears in the studies of small-amplitude gravity waves, Langmuir waves, plane-diffracted waves, Davydov’s alpha-helix waves, and so on.

4. Presentation of methodologies

4.1. The \exp_a function approach

Here, we will give a complete concept of this scheme.

Assuming the nonlinear partial differential equation (PDE),

$$G(q, q^2 q_t, q_x, q_{tt}, q_{xx}, q_{xt}, \dots) = 0. \quad (4.1)$$

Eq (4.3) transformed in nonlinear ordinary differential equation (ODE)

$$\Lambda(Q, Q', Q'', \dots) = 0, \quad (4.2)$$

by using the following transformations:

$$q(x, y, t) = Q(\zeta), \quad \zeta = ax + by + rt. \quad (4.3)$$

Considering the root of Eq (4.2), which is shown in [50–53]:

$$Q(\zeta) = \frac{\alpha_0 + \alpha_1 d^\zeta + \dots + \alpha_m d^{m\zeta}}{\beta_0 + \beta_1 d^\zeta + \dots + \beta_m d^{m\zeta}}, \quad d \neq 0, 1, \quad (4.4)$$

here α_i and β_i ($0 \leq i \leq m$) are undetermined. The positive integral value of m is calculated by utilizing the homogeneous balance technique in Eq (4.2). Substituting Eq (4.4) into Eq (4.2), gives

$$\varphi(d^\zeta) = \ell_0 + \ell_1 d^\zeta + \dots + \ell_t d^{t\zeta} = 0. \quad (4.5)$$

Taking ℓ_i ($0 \leq i \leq t$) in Eq (4.5) equal to 0, a system of algebraic equations is achieved as follows.

$$\ell_i = 0, \quad \text{where } i = 0, \dots, t, \quad (4.6)$$

By using the solutions obtained, we achieve the exact results of Eq (4.1).

4.2. The Sardar sub-equation approach

This part is about the fundamental steps of the Sardar sub-equation method [36]. Assuming the nonlinear fractional partial differential equation given as:

$$F(g, g_t, g_{xx}, g_{xt}, gg_{tt}, g_{xy}, \dots) = 0. \quad (4.7)$$

where $g = g(x, y, t)$ represents a wave profile.

Applying the wave transformations given as follows:

$$g(x, y, t) = G(\zeta), \quad \zeta = \lambda x + \kappa y + \mu t. \quad (4.8)$$

We get a nonlinear ODE given as:

$$Y(G, G'', GG'', G'G^2, \dots) = 0. \quad (4.9)$$

Consider Eq (4.9), which has the solution in the following form:

$$G(\zeta) = \sum_{i=0}^m b_i \psi^i(\zeta). \quad (4.10)$$

where $\psi(\zeta)$ fulfills the ODE given as:

$$\psi'(\zeta) = \sqrt{\sigma + \kappa\psi^2(\zeta) + \psi^4(\zeta)}. \quad (4.11)$$

Here, σ and κ are constants.

Using Eq (4.10) into Eq (4.9) with Eq (4.11) and collecting the coefficients of each power of ψ^i . By putting the coefficient of each power equal to 0, we gain a set of algebraic equations in the terms b_i , λ , μ . By solving the obtained system of equations, we obtain the values of the parameters.

Case 1: If $\kappa > 0$ and $\sigma = 0$, then

$$\psi_1^\pm = \pm \sqrt{-\kappa ab} \operatorname{sech}_{ab}(\sqrt{\kappa} \zeta), \quad (4.12)$$

$$\psi_2^\pm = \pm \sqrt{\kappa ab} \operatorname{csch}_{ab}(\sqrt{\kappa} \zeta), \quad (4.13)$$

where, $\operatorname{sech}_{ab}(\zeta) = \frac{2}{ae^{\zeta} + be^{-\zeta}}$, $\operatorname{csch}_{ab}(\zeta) = \frac{2}{ae^{\zeta} - be^{-\zeta}}$.

Case 2: If $\kappa < 0$ and $\sigma = 0$, then

$$\psi_3^\pm = \pm \sqrt{-\kappa ab} \operatorname{sec}_{ab}(\sqrt{-\kappa} \zeta), \quad (4.14)$$

$$\psi_4^\pm = \pm \sqrt{-\kappa ab} \operatorname{csc}_{ab}(\sqrt{-\kappa} \zeta), \quad (4.15)$$

where, $\operatorname{sec}_{ab}(\zeta) = \frac{2}{ae^{\zeta} + be^{-\zeta}}$, $\operatorname{csc}_{ab}(\zeta) = \frac{2}{ae^{\zeta} - be^{-\zeta}}$.

Case 3: If $\kappa < 0$ and $\sigma = \frac{\kappa^2}{4}$, then

$$\psi_5^\pm = \pm \sqrt{-\frac{\kappa}{2}} \operatorname{tanh}_{ab}(\sqrt{-\frac{\kappa}{2}} \zeta), \quad (4.16)$$

$$\psi_6^\pm = \pm \sqrt{-\frac{\kappa}{2}} \operatorname{coth}_{ab}(\sqrt{-\frac{\kappa}{2}} \zeta), \quad (4.17)$$

$$\psi_7^\pm = \pm \sqrt{-\frac{\kappa}{2}} (\operatorname{tanh}_{ab}(\sqrt{-2\kappa} \zeta) \pm i \sqrt{ab} \operatorname{sech}_{ab}(\sqrt{-2\kappa} \zeta)), \quad (4.18)$$

$$\psi_8^\pm = \pm \sqrt{-\frac{\kappa}{2}} (\operatorname{coth}_{ab}(\sqrt{-2\kappa} \zeta) \pm \sqrt{ab} \operatorname{csch}_{ab}(\sqrt{-2\kappa} \zeta)), \quad (4.19)$$

$$\psi_9^\pm = \pm \sqrt{-\frac{\kappa}{8}} (\operatorname{tanh}_{ab}(\sqrt{-\frac{\kappa}{8}} \zeta) + \operatorname{coth}_{ab}(\sqrt{-\frac{\kappa}{8}} \zeta)), \quad (4.20)$$

where, $\operatorname{tanh}_{ab}(\zeta) = \frac{ae^{\zeta} - be^{-\zeta}}{ae^{\zeta} + be^{-\zeta}}$, $\operatorname{coth}_{ab}(\zeta) = \frac{ae^{\zeta} + be^{-\zeta}}{ae^{\zeta} - be^{-\zeta}}$.

Case 4: If $\kappa > 0$ and $\sigma = \frac{\kappa^2}{4}$, then

$$\psi_{10}^\pm = \pm \sqrt{\frac{\kappa}{2}} \operatorname{tan}_{ab}(\sqrt{\frac{\kappa}{2}} \zeta), \quad (4.21)$$

$$\psi_{11}^{\pm} = \pm \sqrt{\frac{\kappa}{2}} \cot_{ab}(\sqrt{\frac{\kappa}{2}} \zeta), \quad (4.22)$$

$$\psi_{12}^{\pm} = \pm \sqrt{\frac{\kappa}{2}} (\tan_{ab}(\sqrt{2\kappa} \zeta) \pm \sqrt{ab} \sec_{ab}(\sqrt{2\kappa} \zeta)), \quad (4.23)$$

$$\psi_{13}^{\pm} = \pm \sqrt{\frac{\kappa}{2}} (\cot_{ab}(\sqrt{2\kappa} \zeta) \pm \sqrt{ab} \csc_{ab}(\sqrt{2\kappa} \zeta)), \quad (4.24)$$

$$\psi_{14}^{\pm} = \pm \sqrt{\frac{\kappa}{8}} (\tan_{ab}(\sqrt{\frac{\kappa}{8}} \zeta) + \cot_{ab}(\sqrt{\frac{\kappa}{8}} \zeta)), \quad (4.25)$$

where, $\tan_{ab}(\zeta) = -\iota \frac{ae^{i\zeta} - be^{-i\zeta}}{ae^{i\zeta} + be^{-i\zeta}}$, $\cot_{ab}(\zeta) = \iota \frac{ae^{i\zeta} + be^{-i\zeta}}{ae^{i\zeta} - be^{-i\zeta}}$.

4.3. The extended (G'/G) -expansion approach

In this part, there are some fundamental steps of this method given in [22].

Step 1:

Supposing the nonlinear fractional partial differential equation (NLFPDE) is shown as follows:

$$G(q, D_{M,t}^{\alpha,\gamma} q, q^2 q_x, q_y, q_{yy}, q_{xx}, q_{xy}, \dots) = 0, \quad (4.26)$$

Here, $q = q(x, y, t)$ shows the wave function.

Step 2: Assuming the wave transform is shown as follows:

$$q(x, y, t) = Q(\zeta), \quad \zeta = x - vy + \frac{\Gamma(\gamma + 1)}{\alpha} (\kappa t^\alpha), \quad (4.27)$$

Putting Eq (4.27) into Eq (4.26), results in the form of the ordinary differential equation (ODE) shown as:

$$\Lambda(Q(\zeta), Q^2(\zeta)Q'(\zeta), Q''(\zeta), \dots) = 0, \quad (4.28)$$

Step 3:

Considering toots of Eq (4.28) in the form given as:

$$Q(\zeta) = \sum_{i=-m}^m \alpha_i \left(\frac{G'(\zeta)}{G(\zeta)} \right)^i, \quad (4.29)$$

In Eq (4.29), α_0 and α_i , ($i = \pm 1, \pm 2, \pm 3, \dots, \pm m$) are unknowns, and $\alpha_i \neq 0$. Using the homogenous balance method in Eq. (4.28), one can calculate the positive integer m .

The function $G = G(\zeta)$ fulfills the Riccati differential equation shown as follows:

$$dGG'' - aG^2 - bGG' - c(G')^2 = 0, \quad (4.30)$$

where a, b, c, and d are constants.

Step 4:

Suppose Eq (4.30) have results shown as:

Case 1: if $b \neq 0$ and $b^2 + 4ad - 4ac > 0$, then

$$\begin{aligned} \left(\frac{G'(\zeta)}{G(\zeta)} \right) = & \frac{b}{2(d-c)} + \frac{\sqrt{-4ac+4ad+b^2}}{2(d-c)} \\ & \times \left(\frac{C_1 \sinh\left(\frac{\zeta\sqrt{-4ac+4ad+b^2}}{2d}\right) + C_2 \cosh\left(\frac{\zeta\sqrt{-4ac+4ad+b^2}}{2d}\right)}{C_1 \cosh\left(\frac{\zeta\sqrt{-4ac+4ad+b^2}}{2d}\right) + C_2 \sinh\left(\frac{\zeta\sqrt{-4ac+4ad+b^2}}{2d}\right)} \right), \end{aligned} \quad (4.31)$$

Case 2: if $b \neq 0$ and $b^2 + 4ad - 4ac < 0$, then

$$\begin{aligned} \left(\frac{G'(\zeta)}{G(\zeta)} \right) = & \frac{b}{2(d-c)} + \frac{\sqrt{4ac-4ad-b^2}}{2(d-c)} \\ & \times \left(\frac{C_2 \cos\left(\frac{\zeta\sqrt{4ac-4ad-b^2}}{2d}\right) - C_1 \sin\left(\frac{\zeta\sqrt{4ac-4ad-b^2}}{2d}\right)}{C_1 \cos\left(\frac{\zeta\sqrt{4ac-4ad-b^2}}{2d}\right) + C_2 \sin\left(\frac{\zeta\sqrt{4ac-4ad-b^2}}{2d}\right)} \right), \end{aligned} \quad (4.32)$$

Case 3: if $b \neq 0$ and $b^2 + 4ad - 4ac = 0$, then

$$\left(\frac{G'(\zeta)}{G(\zeta)} \right) = \frac{b}{2(d-c)} + \frac{dD}{(d-c)(C-D\zeta)}, \quad (4.33)$$

Case 4: if $b = 0$ and $ad - ac > 0$, then

$$\left(\frac{G'(\zeta)}{G(\zeta)} \right) = \frac{\sqrt{ad-ac}}{(d-c)} \left(\frac{C_1 \sinh\left(\frac{\zeta\sqrt{ad-ac}}{d}\right) + C_2 \cosh\left(\frac{\zeta\sqrt{ad-ac}}{d}\right)}{C_1 \cosh\left(\frac{\zeta\sqrt{ad-ac}}{d}\right) + C_2 \sinh\left(\frac{\zeta\sqrt{ad-ac}}{d}\right)} \right), \quad (4.34)$$

Case 5: if $b = 0$ and $ad - ac < 0$, then

$$\left(\frac{G'(\zeta)}{G(\zeta)} \right) = \frac{\sqrt{ac-ad}}{d-c} \left(\frac{C_2 \cos\left(\frac{\zeta\sqrt{ac-ad}}{d}\right) - C_1 \sin\left(\frac{\zeta\sqrt{ac-ad}}{d}\right)}{C_1 \cos\left(\frac{\zeta\sqrt{ac-ad}}{d}\right) + C_2 \sin\left(\frac{\zeta\sqrt{ac-ad}}{d}\right)} \right), \quad (4.35)$$

where a, b, c, d, C_1 , and C_2 are constants.

Step 5:

Substituting Eq (4.29) along with Eq (4.30) into Eq (4.28) and collecting the coefficients of each power of $\left(\frac{G'(\zeta)}{G(\zeta)}\right)$. By putting each coefficient equal to zero, we achieve a set of algebraic equations involving ν, κ, α_i , ($i = 0, \pm 1, \pm 2, \dots, \pm m$) and other parameters.

Step 6:

Solving the obtained set of equations by using Mathematica software.

Step 7:

Putting the gained solutions into Eq (4.29), we obtain the exact solutions of Eq (4.27).

5. Mathematical analysis

Consider the following traveling wave transformations:

$$g(x, y, z, t) = G(\zeta) \times \exp\left(i\delta\left(\rho x + \mu y + \tau z + \lambda \frac{\Gamma(\varrho+1)}{\epsilon} t^\epsilon\right)\right), \quad (5.1)$$

and

$$\zeta = x + y + z - \omega \frac{\Gamma(\varrho + 1)}{\epsilon} t^\epsilon, \quad (5.2)$$

here, $G(\zeta)$ represents the amplitude of the wave profile, whereas λ and ω are the velocities of solitons, δ denotes a wave number, while ϱ, μ and τ are the other parameters.

By using Eq(5.1) into Eq(3.1), we obtain the real and imaginary parts given as follows:

The real part

$$3G - (\delta^2(\rho^2 + \mu^2 + \tau^2) + \delta\lambda + 2U)G - \theta G^3 = 0, \quad (5.3)$$

and the imaginary part

$$\delta(\rho + \mu + \tau) - \omega = 0, \quad (5.4)$$

From Eq(5.4), we obtain the velocity of solitons, given as:

$$\omega = \delta(\rho + \mu + \tau). \quad (5.5)$$

By utilizing the homogenous balance approach in Eq (5.3), we achieve $m = 1$.

Now we will find the soliton solutions to the above Eq (5.3) by using the described approaches.

5.1. Application to the \exp_a function approach

For $m = 1$, Eq (4.4) changes into

$$G(\zeta) = \frac{\alpha_0 + \alpha_1 d^\zeta}{\beta_0 + \beta_1 d^\zeta}. \quad (5.6)$$

By inserting Eq (5.6) into Eq (5.3) and solving the system of equations, we obtain different solution sets given as follows:

Set 1:

$$\left\{ \alpha_0 = -\frac{\sqrt{\frac{3}{2}}\beta_0 \log(d)}{\sqrt{\theta}}, \alpha_1 = \frac{\sqrt{\frac{3}{2}}\beta_1 \log(d)}{\sqrt{\theta}}, \lambda = -\frac{3 \log^2(d) + 2(\delta^2(\mu^2 + \rho^2 + \tau^2) + 2U)}{2\delta} \right\}, \quad (5.7)$$

$$g_1^I(x, y, z, t) = -\frac{\sqrt{\frac{3}{2}} \log(d)}{\sqrt{\theta}} \left(\frac{\beta_0 - \beta_1 d^{(x+y+z-\delta(\rho+\mu+\tau)\frac{\Gamma(\varrho+1)}{\epsilon}t^\epsilon)}}{\beta_0 + \beta_1 d^{(x+y+z-\delta(\rho+\mu+\tau)\frac{\Gamma(\varrho+1)}{\epsilon}t^\epsilon)}} \right) \\ \times \exp \left(\iota \delta(\rho x + \mu y + \tau z - (\frac{3 \log^2(d) + 2(\delta^2(\mu^2 + \rho^2 + \tau^2) + 2U)}{2\delta}) \frac{\Gamma(\varrho + 1)}{\epsilon} t^\epsilon) \right). \quad (5.8)$$

Set 2:

$$\left\{ \alpha_0 = \frac{\sqrt{\frac{3}{2}}\beta_0 \log(d)}{\sqrt{\theta}}, \alpha_1 = -\frac{\sqrt{\frac{3}{2}}\beta_1 \log(d)}{\sqrt{\theta}}, \lambda = -\frac{3 \log^2(d) + 2(\delta^2(\mu^2 + \rho^2 + \tau^2) + 2U)}{2\delta} \right\}, \quad (5.9)$$

$$g_2^I(x, y, z, t) = \frac{\sqrt{\frac{3}{2}} \log(d)}{\sqrt{\theta}} \left(\frac{\beta_0 - \beta_1 d^{(x+y+z-\delta(\rho+\mu+\tau)\frac{\Gamma(\varrho+1)}{\epsilon}t^\epsilon)}}{\beta_0 + \beta_1 d^{(x+y+z-\delta(\rho+\mu+\tau)\frac{\Gamma(\varrho+1)}{\epsilon}t^\epsilon)}} \right) \\ \times \exp \left(\iota \delta(\rho x + \mu y + \tau z - (\frac{3 \log^2(d) + 2(\delta^2(\mu^2 + \rho^2 + \tau^2) + 2U)}{2\delta}) \frac{\Gamma(\varrho+1)}{\epsilon} t^\epsilon) \right). \quad (5.10)$$

5.2. Application to the SSE approach

For m=1, Eq (4.10) reduces into

$$G(\zeta) = b_0 + b_1 \psi(\zeta) \quad (5.11)$$

Putting Eq (5.11) into Eq (5.3) along Eq (5.12). By summing up the coefficients of each power of $\psi(\zeta)$ and putting them equal to zero, we get a set of algebraic equations. By solving the gained system with the use of the Mathematica tool, we achieve the below solution sets.

Set 1:

$$\left\{ b_0 = 0, b_1 = \pm \frac{\sqrt{6}}{\sqrt{\theta}}, \lambda = \frac{\delta^2(-(\mu^2 + \rho^2 + \tau^2)) + 3\kappa - 2U}{\delta} \right\}, \quad (5.12)$$

$$g_1^{II}(x, y, z, t) = \pm \frac{\sqrt{6}}{\sqrt{\theta}} (\sqrt{-\kappa ab} \operatorname{sech}_{ab}(\sqrt{\kappa} \zeta)) \times \exp \left(\iota \delta(\rho x + \mu y + \tau z + \lambda \frac{\Gamma(\varrho+1)}{\epsilon} t^\epsilon) \right). \quad (5.13)$$

$$g_2^{II}(x, y, z, t) = \pm \frac{\sqrt{6}}{\sqrt{\theta}} (\sqrt{\kappa ab} \operatorname{csch}_{ab}(\sqrt{\kappa} \zeta)) \times \exp \left(\iota \delta(\rho x + \mu y + \tau z + \lambda \frac{\Gamma(\varrho+1)}{\epsilon} t^\epsilon) \right). \quad (5.14)$$

Case 2:

$$g_3^{II}(x, y, z, t) = \pm \frac{\sqrt{6}}{\sqrt{\theta}} (\sqrt{-\kappa ab} \operatorname{sec}_{ab}(\sqrt{-\kappa} \zeta)) \times \exp \left(\iota \delta(\rho x + \mu y + \tau z + \lambda \frac{\Gamma(\varrho+1)}{\epsilon} t^\epsilon) \right). \quad (5.15)$$

$$g_4^{II}(x, y, z, t) = \pm \frac{\sqrt{6}}{\sqrt{\theta}} (\sqrt{-\kappa ab} \operatorname{csc}_{ab}(\sqrt{-\kappa} \zeta)) \times \exp \left(\iota \delta(\rho x + \mu y + \tau z + \lambda \frac{\Gamma(\varrho+1)}{\epsilon} t^\epsilon) \right). \quad (5.16)$$

Case 3:

$$g_5^{II}(x, y, z, t) = \pm \frac{\sqrt{6}}{\sqrt{\theta}} (\sqrt{-\frac{\kappa}{2}} \operatorname{tanh}_{ab}(\sqrt{-\frac{\kappa}{2}} \zeta)) \times \exp \left(\iota \delta(\rho x + \mu y + \tau z + \lambda \frac{\Gamma(\varrho+1)}{\epsilon} t^\epsilon) \right). \quad (5.17)$$

$$g_6^{II}(x, y, z, t) = \pm \frac{\sqrt{6}}{\sqrt{\theta}} (\sqrt{-\frac{\kappa}{2}} \operatorname{coth}_{ab}(\sqrt{-\frac{\kappa}{2}} \zeta)) \times \exp \left(\iota \delta(\rho x + \mu y + \tau z + \lambda \frac{\Gamma(\varrho+1)}{\epsilon} t^\epsilon) \right). \quad (5.18)$$

$$g_7^{II}(x, y, z, t) = \pm \frac{\sqrt{6}}{\sqrt{\theta}} (\sqrt{-\frac{\kappa}{2}} (\operatorname{tanh}_{ab}(\sqrt{-2\kappa} \zeta) \pm \iota \sqrt{ab} \operatorname{sech}_{ab}(\sqrt{-2\kappa} \zeta))) \\ \times \exp \left(\iota \delta(\rho x + \mu y + \tau z + \lambda \frac{\Gamma(\varrho+1)}{\epsilon} t^\epsilon) \right). \quad (5.19)$$

$$g_8^{II}(x, y, z, t) = \pm \frac{\sqrt{6}}{\sqrt{\theta}} \left(\sqrt{-\frac{\kappa}{2}} (\coth_{ab}(\sqrt{-2\kappa}\zeta) \pm \sqrt{ab} \csc_{ab}(\sqrt{-2\kappa}\zeta)) \right. \\ \times \exp \left(\iota \delta(\rho x + \mu y + \tau z + \lambda \frac{\Gamma(\varrho+1)}{\epsilon} t^\epsilon) \right). \quad (5.20)$$

$$g_9^{II}(x, y, z, t) = \pm \frac{\sqrt{6}}{\sqrt{\theta}} \left(\sqrt{-\frac{\kappa}{8}} (\tanh_{ab}(\sqrt{-\frac{\kappa}{8}}\zeta) + \coth_{ab}(\sqrt{-\frac{\kappa}{8}}\zeta)) \right. \\ \times \exp \left(\iota \delta(\rho x + \mu y + \tau z + \lambda \frac{\Gamma(\varrho+1)}{\epsilon} t^\epsilon) \right). \quad (5.21)$$

Case 4

$$g_{10}^{II}(x, y, z, t) = \pm \frac{\sqrt{6}}{\sqrt{\theta}} \left(\sqrt{\frac{\kappa}{2}} \tan_{ab}(\sqrt{\frac{\kappa}{2}}\zeta) \right) \times \exp \left(\iota \delta(\rho x + \mu y + \tau z + \lambda \frac{\Gamma(\varrho+1)}{\epsilon} t^\epsilon) \right). \quad (5.22)$$

$$g_{11}^{II}(x, y, z, t) = \pm \frac{\sqrt{6}}{\sqrt{\theta}} \left(\sqrt{\frac{\kappa}{2}} \cot_{ab}(\sqrt{\frac{\kappa}{2}}\zeta) \right) \times \exp \left(\iota \delta(\rho x + \mu y + \tau z + \lambda \frac{\Gamma(\varrho+1)}{\epsilon} t^\epsilon) \right). \quad (5.23)$$

$$g_{12}^{II}(x, y, z, t) = \pm \frac{\sqrt{6}}{\sqrt{\theta}} \left(\sqrt{\frac{\kappa}{2}} (\tan_{ab}(\sqrt{2\kappa}\zeta) \pm \sqrt{ab} \sec_{ab}(\sqrt{2\kappa}\zeta)) \right. \\ \times \exp \left(\iota \delta(\rho x + \mu y + \tau z + \lambda \frac{\Gamma(\varrho+1)}{\epsilon} t^\epsilon) \right). \quad (5.24)$$

$$g_{13}^{II}(x, y, z, t) = \pm \frac{\sqrt{6}}{\sqrt{\theta}} \left(\sqrt{\frac{\kappa}{2}} (\cot_{ab}(\sqrt{2\kappa}\zeta) \pm \sqrt{ab} \csc_{ab}(\sqrt{2\kappa}\zeta)) \right. \\ \times \exp \left(\iota \delta(\rho x + \mu y + \tau z + \lambda \frac{\Gamma(\varrho+1)}{\epsilon} t^\epsilon) \right). \quad (5.25)$$

$$g_{14}^{II}(x, y, z, t) = \pm \frac{\sqrt{6}}{\sqrt{\theta}} \left(\sqrt{\frac{\kappa}{8}} (\tan_{ab}(\sqrt{\frac{\kappa}{8}}\zeta) + \cot_{ab}(\sqrt{\frac{\kappa}{8}}\zeta)) \right. \\ \times \exp \left(\iota \delta(\rho x + \mu y + \tau z + \lambda \frac{\Gamma(\varrho+1)}{\epsilon} t^\epsilon) \right). \quad (5.26)$$

5.3. Application to the extended (G'/G) -expansion approach

For $m = 1$, Eq (4.29) becomes:

$$G(\zeta) = \alpha_{-1} \left(\frac{G'(\zeta)}{G(\zeta)} \right)^{-1} + \alpha_0 + \alpha_1 \left(\frac{G'(\zeta)}{G(\zeta)} \right). \quad (5.27)$$

here α_{-1}, α_0 and α_1 are unknowns.

Inserting Eq (5.27) along with Eq (4.30) into Eq (5.3) and solving the system for $\alpha_{-1}, \alpha_0, \alpha_1$ and other parameters, we gain different solution sets given as follows:

Set 1:

$$\left\{ \alpha_{-1} = -\frac{\sqrt{6}a}{d\sqrt{\theta}}, \alpha_0 = -\frac{\sqrt{\frac{3}{2}}b}{d\sqrt{\theta}}, \alpha_1 = 0, \lambda = \frac{2(6a(c-d) - d^2(\delta^2(\mu^2 + \rho^2 + \tau^2) + 2U)) - 3b^2}{2d^2\delta} \right\}. \quad (5.28)$$

By using Eqs (5.28), (5.27), (4.31), and (5.1), we achieve

$$\begin{aligned} g_1^{III}(x, y, z, t) &= \frac{-\sqrt{\frac{3}{2}}}{d\sqrt{\theta}}(b + 2a(\frac{b}{2(d-c)} + \frac{\sqrt{4ad-4ac+b^2}}{2(d-c)} \\ &\quad (\frac{C_1 \sinh(\frac{\zeta\sqrt{4ad-4ac+b^2}}{2d}) + C_2 \cosh(\frac{\zeta\sqrt{4ad-4ac+b^2}}{2d}))^{-1}) \\ &\quad (\frac{C_1 \cosh(\frac{\zeta\sqrt{4ad-4ac+b^2}}{2d}) + C_2 \sinh(\frac{\zeta\sqrt{4ad-4ac+b^2}}{2d}))^{-1}) \\ &\times \exp\left(\iota\delta(\rho x + \mu y + \tau z + (\frac{2(6a(c-d) - d^2(\delta^2(\mu^2 + \rho^2 + \tau^2) + 2U)) - 3b^2}{2d^2\delta})\frac{\Gamma(\varrho+1)}{\epsilon}t^\epsilon)\right). \end{aligned} \quad (5.29)$$

By using Eqs (5.28), (5.27), (4.32), and (5.1), we achieve

$$\begin{aligned} g_2^{III}(x, y, z, t) &= -\frac{\sqrt{\frac{3}{2}}}{d\sqrt{\theta}}(b + 2a(\frac{b}{2(d-c)} + \frac{\sqrt{4ac-4ad-b^2}}{2(d-c)} \\ &\quad (\frac{C_2 \cos(\frac{\zeta\sqrt{4ac-4ad-b^2}}{2d}) - C_1 \sin(\frac{\zeta\sqrt{4ac-4ad-b^2}}{2d}))^{-1}) \\ &\quad (\frac{C_1 \cos(\frac{\zeta\sqrt{4ac-4ad-b^2}}{2d}) + C_2 \sin(\frac{\zeta\sqrt{4ac-4ad-b^2}}{2d}))^{-1}) \\ &\times \exp\left(\iota\delta(\rho x + \mu y + \tau z + (\frac{2(6a(c-d) - d^2(\delta^2(\mu^2 + \rho^2 + \tau^2) + 2U)) - 3b^2}{2d^2\delta})\frac{\Gamma(\varrho+1)}{\epsilon}t^\epsilon)\right). \end{aligned} \quad (5.30)$$

By using Eqs (5.28), (5.27), (4.34), and (5.1), we achieve

$$\begin{aligned} g_3^{III}(x, y, z, t) &= -\frac{a\sqrt{6}}{d\sqrt{\theta}}\left(\frac{\sqrt{ad-ac}}{(d-c)}\left(\frac{C_1 \sinh(\frac{\zeta\sqrt{ad-ac}}{d}) + C_2 \cosh(\frac{\zeta\sqrt{ad-ac}}{d})}{C_1 \cosh(\frac{\zeta\sqrt{ad-ac}}{d}) + C_2 \sinh(\frac{\zeta\sqrt{ad-ac}}{d})}\right)\right)^{-1} \\ &\times \exp\left(\iota\delta(\rho x + \mu y + \tau z + (\frac{2(6a(c-d) - d^2(\delta^2(\mu^2 + \rho^2 + \tau^2) + 2U)) - 3b^2}{2d^2\delta})\frac{\Gamma(\varrho+1)}{\epsilon}t^\epsilon)\right). \end{aligned} \quad (5.31)$$

By using Eqs (5.28), (5.27), (4.35), and (5.1), we achieve

$$g_4^{III}(x, y, z, t) = -\frac{a\sqrt{6}}{d\sqrt{\theta}}\left(\frac{\sqrt{ac-ad}}{d-c}\left(\frac{C_2 \cos(\frac{\zeta\sqrt{ac-ad}}{d}) - C_1 \sin(\frac{\zeta\sqrt{ac-ad}}{d})}{C_1 \cos(\frac{\zeta\sqrt{ac-ad}}{d}) + C_2 \sin(\frac{\zeta\sqrt{ac-ad}}{d})}\right)\right)^{-1}$$

$$\times \exp\left(\iota\delta(\rho x + \mu y + \tau z + (\frac{2(6a(c-d) - d^2(\delta^2(\mu^2 + \rho^2 + \tau^2) + 2U))}{2d^2\delta})\frac{\Gamma(\varrho+1)}{\epsilon}t^\epsilon)\right). \quad (5.32)$$

Set 2:

$$\left\{\alpha_{-1} = 0, \alpha_0 = -\frac{\sqrt{\frac{3}{2}}b}{d\sqrt{\theta}}, \alpha_1 = \frac{\sqrt{6}(d-c)}{d\sqrt{\theta}}, \lambda = \frac{2(6a(c-d) - d^2(\delta^2(\mu^2 + \rho^2 + \tau^2) + 2U)) - 3b^2}{2d^2\delta}\right\}. \quad (5.33)$$

By using Eqs (5.33), (5.27), (4.31), and (5.1), we achieve

$$\begin{aligned} g_5^{III}(x, y, z, t) &= \frac{-\sqrt{\frac{3}{2}}}{d\sqrt{\theta}}(b - (b + \sqrt{4ad - 4ac + b^2})) \\ &\quad (\frac{C_1 \sinh(\frac{\zeta\sqrt{4ad-4ac+b^2}}{2d}) + C_2 \cosh(\frac{\zeta\sqrt{4ad-4ac+b^2}}{2d}))}{C_1 \cosh(\frac{\zeta\sqrt{4ad-4ac+b^2}}{2d}) + C_2 \sinh(\frac{\zeta\sqrt{4ad-4ac+b^2}}{2d})) \\ &\times \exp\left(\iota\delta(\rho x + \mu y + \tau z + (\frac{2(6a(c-d) - d^2(\delta^2(\mu^2 + \rho^2 + \tau^2) + 2U)) - 3b^2}{2d^2\delta})\frac{\Gamma(\varrho+1)}{\epsilon}t^\epsilon)\right). \end{aligned} \quad (5.34)$$

By using Eqs (5.33), (5.27), (4.32), and (5.1), we achieve

$$\begin{aligned} g_6^{III}(x, y, z, t) &= \frac{\sqrt{\frac{3}{2}}}{d\sqrt{\theta}}(-b + 2(d-c)(\frac{b}{2(d-c)} + \frac{\sqrt{4ac - 4ad - b^2}}{2(d-c)}) \\ &\quad (\frac{C_2 \cos(\frac{\zeta\sqrt{4ac-4ad-b^2}}{2d}) - C_1 \sin(\frac{\zeta\sqrt{4ac-4ad-b^2}}{2d}))}{C_1 \cos(\frac{\zeta\sqrt{4ac-4ad-b^2}}{2d}) + C_2 \sin(\frac{\zeta\sqrt{4ac-4ad-b^2}}{2d})) \\ &\times \exp\left(\iota\delta(\rho x + \mu y + \tau z + (\frac{2(6a(c-d) - d^2(\delta^2(\mu^2 + \rho^2 + \tau^2) + 2U)) - 3b^2}{2d^2\delta})\frac{\Gamma(\varrho+1)}{\epsilon}t^\epsilon)\right). \end{aligned} \quad (5.35)$$

By using Eqs (5.33), (5.27), (4.34), and (5.1), we achieve

$$\begin{aligned} g_7^{III}(x, y, z, t) &= \frac{\sqrt{6}(d-c)}{d\sqrt{\theta}}\left(\frac{\sqrt{ad-ac}}{(d-c)}\left(\frac{C_1 \sinh\left(\frac{\zeta\sqrt{ad-ac}}{d}\right) + C_2 \cosh\left(\frac{\zeta\sqrt{ad-ac}}{d}\right)}{C_1 \cosh\left(\frac{\zeta\sqrt{ad-ac}}{d}\right) + C_2 \sinh\left(\frac{\zeta\sqrt{ad-ac}}{d}\right)}\right)\right) \\ &\times \exp\left(\iota\delta(\rho x + \mu y + \tau z + (\frac{2(6a(c-d) - d^2(\delta^2(\mu^2 + \rho^2 + \tau^2) + 2U))}{2d^2\delta})\frac{\Gamma(\varrho+1)}{\epsilon}t^\epsilon)\right). \end{aligned} \quad (5.36)$$

By using Eqs (5.33), (5.27), (4.35), and (5.1), we achieve

$$g_8^{III}(x, y, z, t) = \frac{\sqrt{6}(d-c)}{d\sqrt{\theta}}\left(\frac{\sqrt{ac-ad}}{d-c}\left(\frac{C_2 \cos\left(\frac{\zeta\sqrt{ac-ad}}{d}\right) - C_1 \sin\left(\frac{\zeta\sqrt{ac-ad}}{d}\right)}{C_1 \cos\left(\frac{\zeta\sqrt{ac-ad}}{d}\right) + C_2 \sin\left(\frac{\zeta\sqrt{ac-ad}}{d}\right)}\right)\right)$$

$$\times \exp\left(\iota\delta(\rho x + \mu y + \tau z + (\frac{2(6a(c-d) - d^2(\delta^2(\mu^2 + \rho^2 + \tau^2) + 2U))}{2d^2\delta})\frac{\Gamma(\varrho+1)}{\epsilon}t^\epsilon)\right). \quad (5.37)$$

Set 3:

$$\left\{\alpha_{-1} = \frac{\sqrt{6}a}{d\sqrt{\theta}}, \alpha_0 = \frac{\sqrt{\frac{3}{2}}b}{d\sqrt{\theta}}, \alpha_1 = 0, \lambda = \frac{2(6a(c-d) - d^2(\delta^2(\mu^2 + \rho^2 + \tau^2) + 2U)) - 3b^2}{2d^2\delta}\right\}. \quad (5.38)$$

By using Eqs (5.38), (5.27), (4.31), and (5.1), we achieve

$$g_9^{III}(x, y, z, t) = \frac{\sqrt{\frac{3}{2}}}{d\sqrt{\theta}}(b + 2a(\frac{b}{2(d-c)} + \frac{\sqrt{4ad - 4ac + b^2}}{2(d-c)}) \\ (\frac{C_1 \sinh(\frac{\zeta\sqrt{4ad-4ac+b^2}}{2d}) + C_2 \cosh(\frac{\zeta\sqrt{4ad-4ac+b^2}}{2d})}{C_1 \cosh(\frac{\zeta\sqrt{4ad-4ac+b^2}}{2d}) + C_2 \sinh(\frac{\zeta\sqrt{4ad-4ac+b^2}}{2d}))^{-1}) \\ \times \exp\left(\iota\delta(\rho x + \mu y + \tau z + (\frac{2(6a(c-d) - d^2(\delta^2(\mu^2 + \rho^2 + \tau^2) + 2U)) - 3b^2}{2d^2\delta})\frac{\Gamma(\varrho+1)}{\epsilon}t^\epsilon)\right). \quad (5.39)$$

By using Eqs (5.38), (5.27), (4.32), and (5.1), we achieve

$$g_{10}^{III}(x, y, z, t) = \frac{\sqrt{\frac{3}{2}}}{d\sqrt{\theta}}(b + 2a(\frac{b}{2(d-c)} + \frac{\sqrt{4ac - 4ad - b^2}}{2(d-c)}) \\ (\frac{C_2 \cos(\frac{\zeta\sqrt{4ac-4ad-b^2}}{2d}) - C_1 \sin(\frac{\zeta\sqrt{4ac-4ad-b^2}}{2d})}{C_1 \cos(\frac{\zeta\sqrt{4ac-4ad-b^2}}{2d}) + C_2 \sin(\frac{\zeta\sqrt{4ac-4ad-b^2}}{2d}))^{-1}) \\ \times \exp\left(\iota\delta(\rho x + \mu y + \tau z + (\frac{2(6a(c-d) - d^2(\delta^2(\mu^2 + \rho^2 + \tau^2) + 2U)) - 3b^2}{2d^2\delta})\frac{\Gamma(\varrho+1)}{\epsilon}t^\epsilon)\right). \quad (5.40)$$

By using Eqs (5.38), (5.27), (4.34), and (5.1), we achieve

$$g_{11}^{III}(x, y, z, t) = \frac{a\sqrt{6}}{d\sqrt{\theta}}\left(\frac{\sqrt{ad-ac}}{(d-c)}\left(\frac{C_1 \sinh(\frac{\zeta\sqrt{ad-ac}}{d}) + C_2 \cosh(\frac{\zeta\sqrt{ad-ac}}{d})}{C_1 \cosh(\frac{\zeta\sqrt{ad-ac}}{d}) + C_2 \sinh(\frac{\zeta\sqrt{ad-ac}}{d})}\right)\right)^{-1} \\ \times \exp\left(\iota\delta(\rho x + \mu y + \tau z + (\frac{2(6a(c-d) - d^2(\delta^2(\mu^2 + \rho^2 + \tau^2) + 2U))}{2d^2\delta})\frac{\Gamma(\varrho+1)}{\epsilon}t^\epsilon)\right). \quad (5.41)$$

By using Eqs (5.38), (5.27), (4.35), and (5.1), we achieve

$$g_{12}^{III}(x, y, z, t) = \frac{a\sqrt{6}}{d\sqrt{\theta}} \left(\frac{\sqrt{ac-ad}}{d-c} \left(\frac{C_2 \cos\left(\frac{\zeta\sqrt{ac-ad}}{d}\right) - C_1 \sin\left(\frac{\zeta\sqrt{ac-ad}}{d}\right)}{C_1 \cos\left(\frac{\zeta\sqrt{ac-ad}}{d}\right) + C_2 \sin\left(\frac{\zeta\sqrt{ac-ad}}{d}\right)} \right) \right)^{-1} \\ \times \exp \left(\iota \delta (\rho x + \mu y + \tau z + \left(\frac{2(6a(c-d) - d^2(\delta^2(\mu^2 + \rho^2 + \tau^2) + 2U))}{2d^2\delta} \right) \frac{\Gamma(\varrho+1)}{\epsilon} t^\epsilon) \right). \quad (5.42)$$

Set 4:

$$\left\{ \alpha_{-1} = 0, \alpha_0 = \frac{\sqrt{\frac{3}{2}} b}{d\sqrt{\theta}}, \alpha_1 = \frac{\sqrt{6}(c-d)}{d\sqrt{\theta}}, \lambda = \frac{2(6a(c-d) - d^2(\delta^2(\mu^2 + \rho^2 + \tau^2) + 2U)) - 3b^2}{2d^2\delta} \right\}. \quad (5.43)$$

By using Eqs (5.43), (5.27), (4.31), and (5.1), we achieve

$$g_{13}^{III}(x, y, z, t) = \frac{\sqrt{\frac{3}{2}}}{d\sqrt{\theta}} (b + 2(c-d) \left(\frac{b}{2(d-c)} + \frac{\sqrt{4ad-4ac+b^2}}{2(d-c)} \right. \\ \left. \left(\frac{C_1 \sinh(\frac{\zeta\sqrt{4ad-4ac+b^2}}{2d}) + C_2 \cosh(\frac{\zeta\sqrt{4ad-4ac+b^2}}{2d})}{C_1 \cosh(\frac{\zeta\sqrt{4ad-4ac+b^2}}{2d}) + C_2 \sinh(\frac{\zeta\sqrt{4ad-4ac+b^2}}{2d})} \right) \right) \\ \times \exp \left(\iota \delta (\rho x + \mu y + \tau z + \left(\frac{2(6a(c-d) - d^2(\delta^2(\mu^2 + \rho^2 + \tau^2) + 2U)) - 3b^2}{2d^2\delta} \right) \frac{\Gamma(\varrho+1)}{\epsilon} t^\epsilon) \right). \quad (5.44)$$

By using Eqs (5.43), (5.27), (4.32), and (5.1), we achieve

$$g_{14}^{III}(x, y, z, t)(x, y, z, t) = \frac{\sqrt{\frac{3}{2}}}{d\sqrt{\theta}} (b + 2(c-d) \left(\frac{b}{2(d-c)} + \frac{\sqrt{4ac-4ad-b^2}}{2(d-c)} \right. \\ \left. \left(\frac{C_2 \cos(\frac{\zeta\sqrt{4ac-4ad-b^2}}{2d}) - C_1 \sin(\frac{\zeta\sqrt{4ac-4ad-b^2}}{2d})}{C_1 \cos(\frac{\zeta\sqrt{4ac-4ad-b^2}}{2d}) + C_2 \sin(\frac{\zeta\sqrt{4ac-4ad-b^2}}{2d})} \right) \right) \\ \times \exp \left(\iota \delta (\rho x + \mu y + \tau z + \left(\frac{2(6a(c-d) - d^2(\delta^2(\mu^2 + \rho^2 + \tau^2) + 2U)) - 3b^2}{2d^2\delta} \right) \frac{\Gamma(\varrho+1)}{\epsilon} t^\epsilon) \right). \quad (5.45)$$

By using Eqs (5.43), (5.27), (4.34), and (5.1), we achieve

$$g_{15}^{III}(x, y, z, t) = \frac{\sqrt{6}(c-d)}{d\sqrt{\theta}} \left(\frac{\sqrt{ad-ac}}{(d-c)} \left(\frac{C_1 \sinh(\frac{\zeta\sqrt{ad-ac}}{d}) + C_2 \cosh(\frac{\zeta\sqrt{ad-ac}}{d})}{C_1 \cosh(\frac{\zeta\sqrt{ad-ac}}{d}) + C_2 \sinh(\frac{\zeta\sqrt{ad-ac}}{d})} \right) \right) \\ \times \exp \left(\iota \delta (\rho x + \mu y + \tau z + \left(\frac{2(6a(c-d) - d^2(\delta^2(\mu^2 + \rho^2 + \tau^2) + 2U))}{2d^2\delta} \right) \frac{\Gamma(\varrho+1)}{\epsilon} t^\epsilon) \right). \quad (5.46)$$

By using Eqs (5.43), (5.27), (4.35), and (5.1), we achieve

$$g_{16}^{III}(x, y, z, t) = \frac{\sqrt{6}(c-d)}{d\sqrt{\theta}} \left(\frac{\sqrt{ac-ad}}{d-c} \left(\begin{array}{l} C_2 \cos\left(\frac{\zeta\sqrt{ac-ad}}{d}\right) - C_1 \sin\left(\frac{\zeta\sqrt{ac-ad}}{d}\right) \\ C_1 \cos\left(\frac{\zeta\sqrt{ac-ad}}{d}\right) + C_2 \sin\left(\frac{\zeta\sqrt{ac-ad}}{d}\right) \end{array} \right) \right) \times \exp\left(\iota\delta(\rho x + \mu y + \tau z + \left(\frac{2(6a(c-d) - d^2(\delta^2(\mu^2 + \rho^2 + \tau^2) + 2U))}{2d^2\delta} \right) \frac{\Gamma(\varrho+1)}{\epsilon} t^\varrho \right) \right). \quad (5.47)$$

6. Discussion and results

In this section, the graphical representations of the truncated M-fractional (3+1)-dimensional Gross–Pitaevskii equation with periodic potential have been illustrated. The 3D, contour, and 2D graphs visualize the nature of nonlinear waves constructed from Eq (2.1). A family of bright, dark, periodic, and singular solitons is displayed for a set of values. A more detailed comprehension of the dynamical wave structures is presented in the two- and three-dimensional graphs of the computed results using different variable selections. It has been noted that certain periodic wave solutions can depict oscillatory or periodic motion, albeit oscillatory motion is restricted to oscillating between two states or around an equilibrium point. Every movement that happens repeatedly throughout time is considered periodic motion. The solitary wave forms that depict the nature of the solution as the blow-up period approaches are another form of the created wave structures, and they are incredibly intriguing to visualize through various wave shapes. The singularity assumes a simple form when the solution becomes unbounded in finite time. When the solution is still bounded, we can say that the wave has broken even though its slope becomes infinite in finite time. The graph gradually becomes steeper as it propagates, until it reaches a point where the slope is vertical and the wave is considered to have broken.

By employing the \exp_a function approach: Figure 1 illustrates a dark singular wave soliton $g_1^I(x, y, z, t)$ observed for Case-I when $\beta_0 = 4, \beta_1 = 2, \epsilon = 1, \delta = 0.25, \theta = 45, \lambda = 3, \mu = 2, \rho = 1, \tau = 2, d = 10, t = 1, z = 2$. While Figure 2 demonstrates a dark solitary wave $g_2^I(x, y, z, t)$ developed when $\beta_0 = 3, \beta_1 = 4, \epsilon = 1, \delta = 0.25, \theta = 90, \lambda = 1, \mu = 2, \rho = 1, \tau = 0.5, d = 2, t = 1, z = 2$.

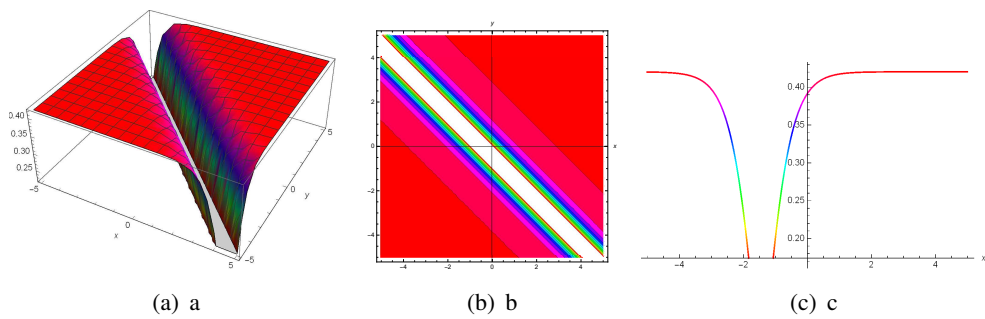


Figure 1. 3D, contour, and 2D plots for $|g_1^I(x, y, z, t)|$ when $\beta_0 = 4, \beta_1 = 2, \epsilon = 1, \delta = 0.25, \theta = 45, \lambda = 3, \mu = 2, \rho = 1, \tau = 2, d = 10, t = 1, z = 2$.

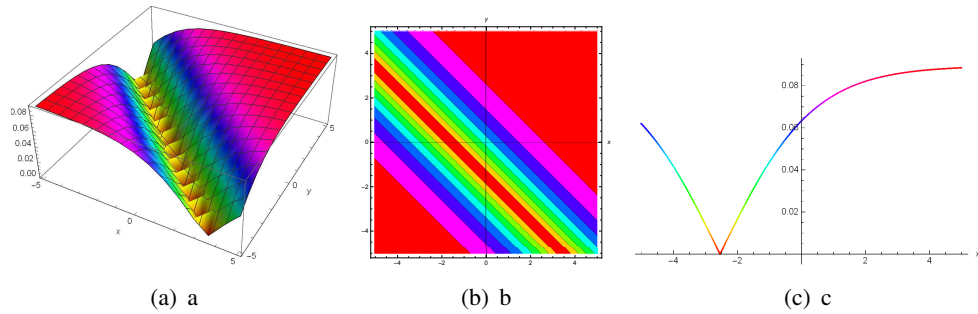


Figure 2. 3D, contour, and 2D plots for $|g_2^I(x, y, z, t)|$ when $\beta_0 = 3$, $\beta_1 = 4$, $\epsilon = 1$, $\delta = 0.25$, $\theta = 90$, $\lambda = 1$, $\mu = 2$, $\rho = 1$, $\tau = 0.5$, $d = 2$, $t = 1$, $z = 2$.

Similarly, implementing the SSE technique: Figure 3 depicts a bell-shaped bright soliton $g_2^{II}(x, y, t)$ for $\epsilon = 1$, $\delta = 0.25$, $\theta = 45$, $\kappa = 2$, $\mu = 1$, $\rho = 1$, $\tau = 2$, $a = 3$, $b = 2$, $t = 1$, $z = 1$, while Figure 4 illustrates a singular wave structure $g_4^{II}(x, y, z, t)$ for $\epsilon = 1$, $\delta = 0.25$, $\theta = 45$, $\kappa = 2$, $\mu = 1$, $\rho = 1$, $\tau = 2$, $a = 3$, $b = 2$, $t = 1$, $z = 1$.

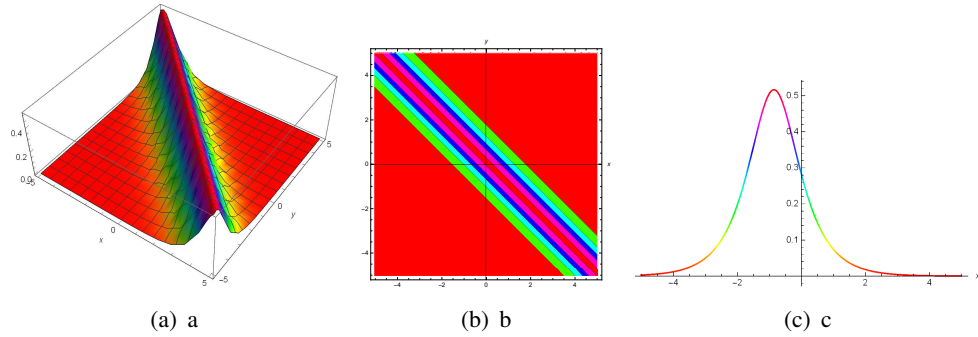


Figure 3. 3D, contour, and 2D plots for $|g_1^{II}(x, y, z, t)|$ when $\epsilon = 1$, $\delta = 0.25$, $\theta = 45$, $\kappa = 2$, $\mu = 1$, $\rho = 1$, $\tau = 2$, $a = 3$, $b = 2$, $t = 1$, $z = 1$.

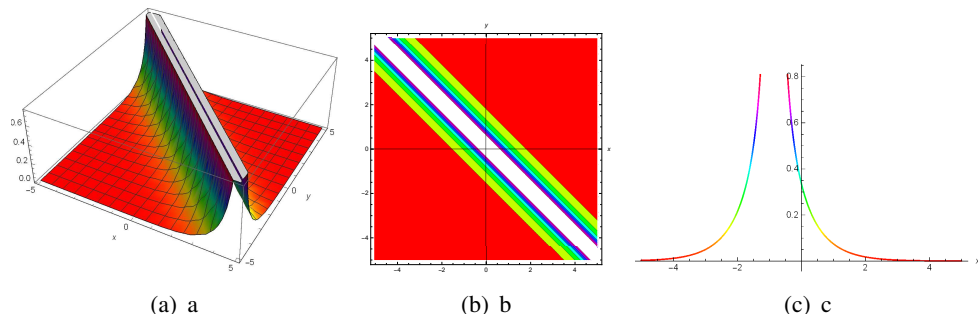


Figure 4. 3D, contour, and 2D plots for $|g_4^{II}(x, y, z, t)|$ when $\epsilon = 1$, $\delta = 0.25$, $\theta = 45$, $\kappa = 2$, $\mu = 1$, $\rho = 1$, $\tau = 2$, $a = 3$, $b = 2$, $t = 1$, $z = 1$.

Figure 5 displays a periodic wave $g_6^{II}(x, y, z, t)$ observed for $\epsilon = 3$, $\delta = 1$, $\theta = 90$, $\kappa = 0.25$, $\mu = 0.5$, $\rho = 1$, $\tau = 2$, $a = 1$, $b = -2$, $t = 1$, $z = 1$. Figure 6 expresses a periodic wave structure $g_9^{II}(x, y, z, t)$ for $\epsilon = 1$, $\delta = 0.25$, $\theta = 45$, $\kappa = 2$, $\mu = 1$, $\rho = 1$, $\tau = 2$, $a = 3$, $b = 2$, $t = 1$, $z = 1$.

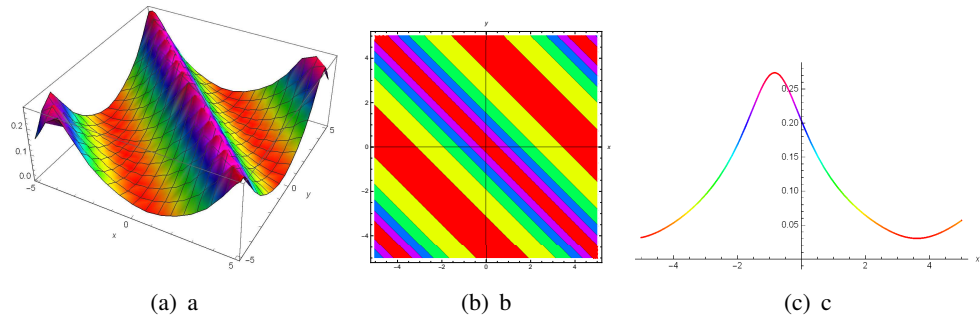


Figure 5. 3D, contour, and 2D plots for $|g_6^{II}(x, y, z, t)|$ when $\epsilon = 3$, $\delta = 1$, $\theta = 90$, $\kappa = 0.25$, $\mu = 0.5$, $\rho = 1$, $\tau = 2$, $a = 1$, $b = -2$, $t = 1$, $z = 1$.

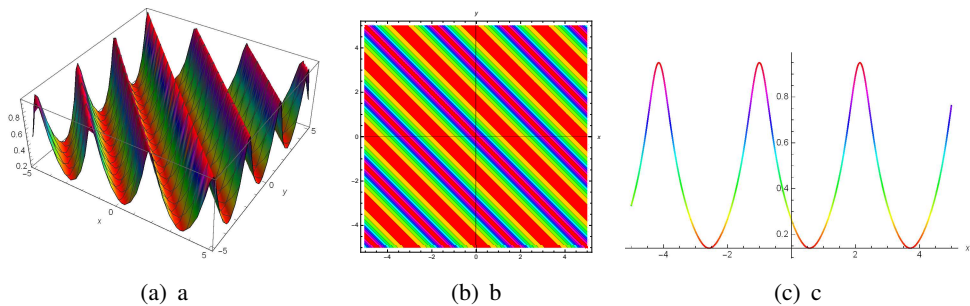


Figure 6. 3D, contour, and 2D plots for $|g_9^H(x, y, z, t)|$ when $\epsilon = 1, \delta = 0.25, \theta = 45, \kappa = 2, \mu = 1, \rho = 1, \tau = 2, a = 3, b = 2, t = 1, z = 1$.

Furthermore, applying the (G'/G) -expansion method: Figure 7 depicts a bell shaped soliton $g_1^{III}(x, y, z, t)$ for $\epsilon = 1$, $\delta = 1$, $\theta = 45$, $\rho = 2$, $\kappa = 1$, $a = 3$, $b = 2$, $t = 1$, while Figure 7 illustrates a periodic soliton $g_3^{III}(x, y, z, t)$ for $\epsilon = 2$, $\delta = 0.5$, $\theta = 90$, $\kappa = 0.25$, $\mu = -2$, $\rho = 1$, $\tau = 3$, $a = 3$, $b = 2$, $t = 1$, $z = 1$.

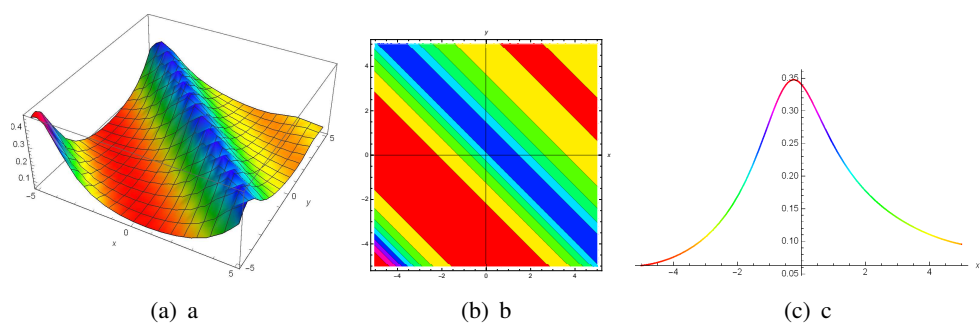


Figure 7. 3D, contour, and 2D plots for $|g_1^{III}(x, y, z, t)|$ when $\epsilon = 2, \delta = 0.5, \theta = 90, \kappa = 0.25, \mu = -2, \rho = 1, \tau = 3, a = 3, b = 2, t = 1, z = 1$.

Whereas Figure 8 displays a soliatory wave $g_2^{III}(x, y, z, t)$ for $\epsilon = 1$, $\delta = 0.25$, $\theta = 9$, $\kappa = 2$, $\mu = 1$, $\rho = 1$, $\tau = 3$, $a = 0.5$, $b = 2$, $c = 3$, $C_1 = 1$, $C_2 = 2$, $d = 4$, $t = 1$, $z = 1$ then Figure 9 expresses a singular soliton $g_7^{III}(x, y, z, t)$ for $\epsilon = 1$, $\delta = 0.25$, $\theta = 5$, $\kappa = 2$, $\mu = 1$, $\rho = 1$, $\tau = 2$, $a = 5$, $b = 2$, $c = 3$, $C_1 = 1$, $C_2 = 2$, $d = 4$, $t = 1$, $z = 1$.

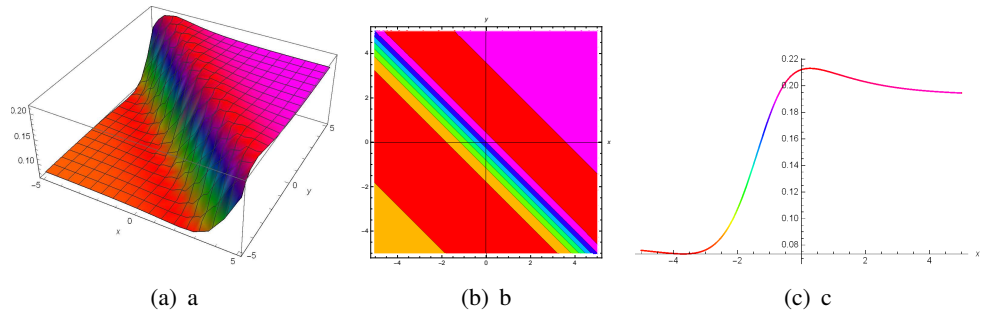


Figure 8. 3D, contour, and 2D plots for $|g_2^{III}(x, y, z, t)|$ when $\epsilon = 1, \delta = 0.25, \theta = 9, \kappa = 2, \mu = 1, \rho = 1, \tau = 3, a = 0.5, b = 2, c = 3, C_1 = 1, C_2 = 2, d = 4, t = 1, z = 1$.

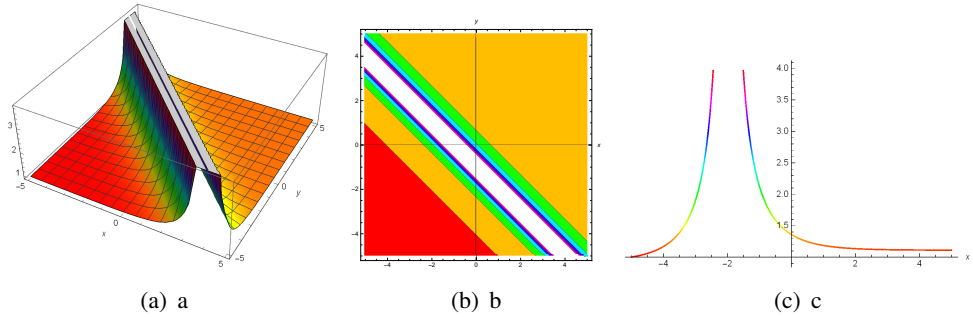


Figure 9. 3D, contour, and 2D plots for $|g_7^{III}(x, y, z, t)|$ when $\epsilon = 1, \delta = 0.25, \theta = 5, \kappa = 2, \mu = 1, \rho = 1, \tau = 2, a = 5, b = 2, c = 3, C_1 = 1, C_2 = 2, d = 4, t = 1, z = 1$.

While Figure 10 expresses a bright wave $g_{10}^{III}(x, y, z, t)$ for $\epsilon = 1$, $\delta = 0.25$, $\theta = 5$, $\kappa = 2$, $\mu = 1$, $\rho = 1$, $\tau = 2$, $a = 5$, $b = 2$, $c = 3$, $C_1 = 1$, $C_2 = 2$, $d = 4$, $t = 1$, $z = 1$, whereas Figure 11 expresses a solitary wave structure $g_{14}^{III}(x, y, z, t)$ for $\epsilon = 1$, $\delta = 0.25$, $\theta = 4$, $\kappa = 2$, $\mu = 1$, $\rho = 1$, $\tau = 2$, $a = 3$, $b = 5$, $c = 2$, $d = 1$, $t = 1$, $z = 1$, and Figure 12 expresses a solitary wave structure $g_{16}^{III}(x, y, z, t)$ for $\epsilon = 1$, $\delta = 0.25$, $\theta = 4$, $\kappa = 2$, $\mu = 1$, $\rho = 1$, $\tau = 2$, $a = 1$, $b = 2$, $c = -3$, $C_1 = 3$, $C_2 = 2$, $d = 1$, $t = 1$, $z = 1$.

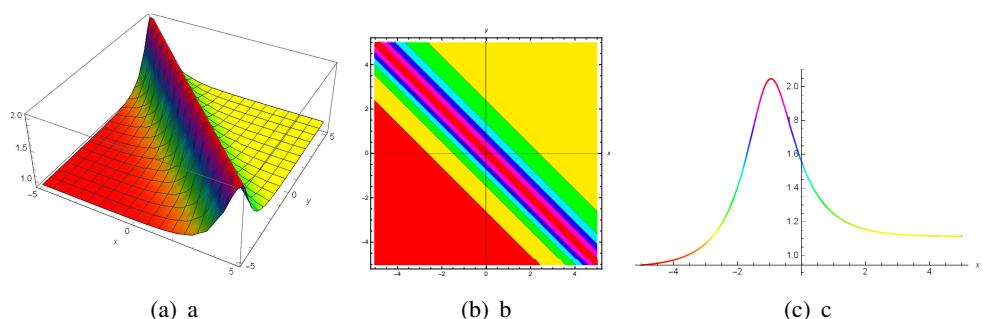


Figure 10. 3D, contour, and 2D plots for $|g_{10}^{III}(x, y, z, t)|$ when $\epsilon = 1$, $\delta = 0.25$, $\theta = 5$, $\kappa = 2$, $\mu = 1$, $\rho = 1$, $\tau = 2$, $a = 5$, $b = 2$, $c = 3$, $C_1 = 1$, $C_2 = 2$, $d = 4$, $t = 1$, $z = 1$.

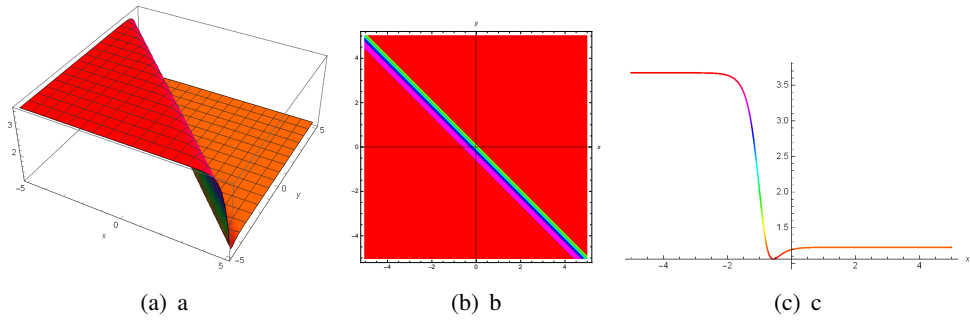


Figure 11. 3D, contour, and 2D plots for $|g_{14}^{III}(x, y, z, t)|$ when $\epsilon = 2, \delta = 0.5, \theta = 90, \kappa = 0.25, \mu = -2, \rho = 1, \tau = 3, a = 3, b = 2, t = 1, z = 1$.

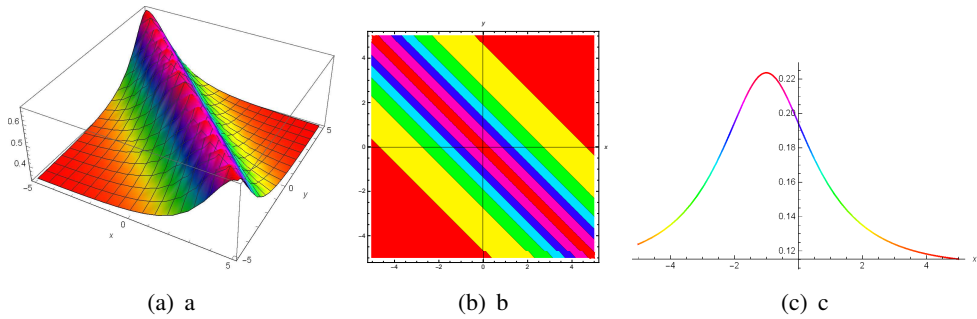


Figure 12. 3D, contour, and 2D plots for $|g_{16}^{III}(x, y, z, t)|$ when $\epsilon = 1, \delta = 0.25, \theta = 4, \kappa = 2, \mu = 1, \rho = 1, \tau = 2, a = 1, b = 2, c = -3, C_1 = 3, C_2 = 2, d = 1, t = 1, z = 1$.

7. Conclusions

We have succeeded in obtaining the modernistic soliton solutions of the truncated M-fractional (3+1)-dimensional periodic potential Gross–Pitaevskii equation by utilizing the \exp_a function approach, the Sardar sub-equation approach, and the extended (G'/G) -expansion approach. The solutions are also verified and demonstrated through visualization using MATHEMATICA software. Finally, it is suggested that to deal with the other nonlinear partial differential equations, the applied strategies are very helpful, reliable, and straight-forward. An interesting fact about paper is that, first, a new definition of derivative is used for this model. The obtained results may be helpful in future research on the model. A variety of behaviors are seen in the observed solutions, such as optical soliton solutions and dark, bright, singular, periodic, and bell-shaped ones. Because of how extremely significant and credible the results are in explaining a range of physical circumstances, this study is more valuable. Graphs using contour plots, 2D, and 3D can also be used to display the established results; for details, see Figures 1–12. Many natural phenomena, such as fluid dynamics, wave motion; and optical fiber characteristics, are illustrated by these solutions in terms of their physical behavior. The employed methodologies have been demonstrated to be beneficial and helpful in handling several other nonlinear fractional models found in fluid dynamics, hydrodynamics, plasma, and other scientific and engineering fields.

Use of AI tools declaration

The authors declare they have not used Artificial Intelligence (AI) tools in the creation of this article.

Author contributions

H.Q.: Methodology, conceptualization, validation, writing original draft. A.A.: Formal analysis and investigation, funding acquisition, writing original draft. A.B.: Supervision, project administration, review and editing. K.U.T.: Software, methodology, visualization, writing original draft.

Acknowledgments

The authors extend their appreciation to Prince Sattam bin Abdulaziz University for funding this research work through the project number (PSAU/2024/01/921063).

Conflict of interest

The authors declare that they have no competing interests.

References

1. A. Neirameh, M. Eslami, New solitary wave solutions for fractional Jaulent–Miodek hierarchy equation, *Mod. Phys. Lett. B*, **36** (2022), 2150612. <https://doi.org/10.1142/S0217984921506120>
2. H. Rezazadeh, M. S. Osman, M. Eslami, M. Ekici, A. Sonmezoglu, M. Asma, et al., Mitigating internet bottleneck with fractional temporal evolution of optical solitons having quadratic–cubic nonlinearity, *Optik*, **164** (2018), 84–92. <https://doi.org/10.1016/j.ijleo.2018.03.006>
3. M. S. Osman, One-soliton shaping and inelastic collision between double solitons in the fifth-order variable-coefficient Sawada–Kotera equation, *Nonlinear Dyn.*, **96** (2019), 1491–1496. <https://doi.org/10.1007/s11071-019-04866-1>
4. F. Badshah, K. U. Tariq, M. Inc, F. Mehboob, On lump, travelling wave solutions and the stability analysis for the (3+1)-dimensional nonlinear fractional generalized shallow water wave model in fluids, *Opt. Quant. Electron.*, **56** (2024), 244. <https://doi.org/10.1007/s11082-023-05826-1>
5. K. K. Ali, A. Wazwaz, M. S. Osman, Optical soliton solutions to the generalized nonautonomous nonlinear Schrödinger equations in optical fibers via the sine-Gordon expansion method, *Optik*, **208** (2020), 164132. <https://doi.org/10.1016/j.ijleo.2019.164132>
6. M. S. Aktar, M. A. Akbar, M. S. Osman, Spatio-temporal dynamic solitary wave solutions and diffusion effects to the nonlinear diffusive predator-prey system and the diffusion-reaction equations, *Chaos Soliton. Fract.*, **160** (2022), 112212. <https://doi.org/10.1016/j.chaos.2022.112212>
7. B. Inan, M. S. Osman, A. k. Turgut, D. Baleanu, Analytical and numerical solutions of mathematical biology models: The Newell–Whitehead–Segel and Allen–Cahn equations, *Math. method. Appl. Sci.*, **43** (2020), 2588–2600. <https://doi.org/10.1002/mma.6067>

8. M. Adel, D. Baleanu, U. Sadiya, M. A. Arefin, M. H. Uddin, M. A. Elamin, et al., Inelastic soliton wave solutions with different geometrical structures to fractional order nonlinear evolution equations, *Results in Physics*, **38** (2022), 105661. <https://doi.org/10.1016/j.rinp.2022.105661>
9. S. Kumar, S. K. Dhiman, D. Baleanu, M. S. Osman, A. Wazwaz, Lie symmetries, closed-form solutions, and various dynamical profiles of solitons for the variable coefficient (2+1)-dimensional KP equations, *Symmetry*, **14** (2022), 597. <https://doi.org/10.3390/sym14030597>
10. F. Badshah, K. U. Tariq, A. Bekir, R. N. Tufail, H. Ilyas, Lump, periodic, travelling, semi-analytical solutions and stability analysis for the Ito integro-differential equation arising in shallow water waves, *Chaos Soliton. Fract.*, **182** (2024), 114783. <https://doi.org/10.1016/j.chaos.2024.114783>
11. K. K. Ali, R. Yilmazer, M. S. Osman, Dynamic behavior of the (3+1)-dimensional KdV–Calogero–Bogoyavlenskii–Schiff equation, *Opt. Quant. Electron.*, **54** (2022), 160. <https://doi.org/10.1007/s11082-022-03528-8>
12. S. Tarla, K. K. Ali, R. Yilmazer, M. S. Osman, The dynamic behaviors of the Radhakrishnan–Kundu–Lakshmanan equation by Jacobi elliptic function expansion technique, *Opt. Quant. Electron.*, **54** (2022), 292. <https://doi.org/10.1007/s11082-022-03710-y>
13. S. Rashid, K. T. Kubra, S. Sultana, P. Agarwal, M. S. Osman, An approximate analytical view of physical and biological models in the setting of Caputo operator via Elzaki transform decomposition method, *J. Comput. Appl. Math.*, **413** (2022), 114378. <https://doi.org/10.1016/j.cam.2022.114378>
14. H. F. Ismael, I. Okumuş, T. Aktürk, H. Bulut, M. S. Osman, Analyzing study for the 3D potential Yu–Toda–Sasa–Fukuyama equation in the two-layer liquid medium, *J. Ocean Eng. Sci.*, 2022. In press. <https://doi.org/10.1016/j.joes.2022.03.017>
15. A. R. Seadawy, N. Cheemaa, A. Biswas, Optical dromions and domain walls in (2+1)-dimensional coupled system, *Optik*, **227** (2021), 165669. <https://doi.org/10.1016/j.ijleo.2020.165669>
16. S. El-Ganaini, M. O. Al-Amr, New abundant solitary wave structures for a variety of some nonlinear models of surface wave propagation with their geometric interpretations, *Math. Method. Appl. Sci.*, **45** (2022), 7200–7226. <https://doi.org/10.1002/mma.8232>
17. M. O. Al-Amr, H. Rezazadeh, K. K. Ali, A. Korkmaz, N1-soliton solution for Schrödinger equation with competing weakly nonlocal and parabolic law nonlinearities, *Commun. Theor. Phys.*, **72** (2020), 065503. <https://doi.org/10.1088/1572-9494/ab8a12>
18. M. N. Rasheed, M. O. Al-Amr, E. A. Az-Zo’bi, M. A. Tashtoush, L. Akinyemi, Stable optical solitons for the Higher-order Non-Kerr NLSE via the modified simple equation method, *Mathematics*, **9** (2021) 1986. <https://doi.org/10.3390/math9161986>
19. M. Eslami, H. Rezazadeh, The first integral method for Wu–Zhang system with conformable time-fractional derivative, *Calcolo*, **53** (2016), 475–485. <https://doi.org/10.1007/s10092-015-0158-8>
20. H. Rezazadeh, D. Kumar, A. Neirameh, M. Eslami, M. Mirzazadeh, Applications of three methods for obtaining optical soliton solutions for the Lakshmanan–Porsezian–Daniel model with Kerr law nonlinearity, *Pramana*, **94** (2020), 39. <https://doi.org/10.1007/s12043-019-1881-5>

21. A. Zafar, M. Raheel, M. Mirzazadeh, M. Eslami, Different soliton solutions to the modified equal-width wave equation with Beta-time fractional derivative via two different methods, *Rev. Mex. Fis.*, **68** (2022), 010701. <https://doi.org/10.31349/revmexfis.68.010701>
22. S. Sahoo, S. S. Ray, M. A. Abdou, New exact solutions for time-fractional Kaup-Kupershmidt equation using improved (G'/G) -expansion and extended (G'/G) -expansion methods, *Alex. Eng. J.*, **59** (2020), 3105–3110. <https://doi.org/10.1016/j.aej.2020.06.043>
23. Z. Zou, R. Guo, The Riemann–Hilbert approach for the higher-order Gerdjikov–Ivanov equation, soliton interactions and position shift, *Commun. Nonlinear Sci.*, **124** (2023), 107316. <https://doi.org/10.1016/j.cnsns.2023.107316>
24. N. Nasreen, U. Younas, T. A. Sulaiman, Z. Zhang, D. Lu, A variety of M-truncated optical solitons to a nonlinear extended classical dynamical model, *Results Phys.*, **51** (2023), 106722. <https://doi.org/10.1016/j.rinp.2023.106722>
25. F. Badshah, K. U. Tariq, A. Bekir, S. M. R. Kazmi, Stability, modulation instability and wave solutions of time-fractional perturbed nonlinear Schrödinger model, *Opt. Quant. Electron.*, **56** (2024), 425. <https://doi.org/10.1007/s11082-023-06058-z>
26. O. M. Braun, Y. S. Kivshar, Nonlinear dynamics of the Frenkel–Kontorova model, *Phys. Rep.*, **306** (1998), 1–108. [https://doi.org/10.1016/S0370-1573\(98\)00029-5](https://doi.org/10.1016/S0370-1573(98)00029-5)
27. S. Shen, Z. J. Yang, Z. G. Pang, Y. R. Ge, The complex-valued astigmatic cosine-Gaussian soliton solution of the nonlocal nonlinear Schrödinger equation and its transmission characteristics, *Appl. Math. Lett.*, **125** (2022), 107755. <https://doi.org/10.1016/j.aml.2021.107755>
28. L. M. Song, Z. J. Yang, X. L. Li, S. M. Zhang, Coherent superposition propagation of Laguerre–Gaussian and Hermite–Gaussian solitons, *Appl. Math. Lett.*, **102** (2020), 106114. <https://doi.org/10.1016/j.aml.2019.106114>
29. S. Shen, Z. J. Yang, X. L. Li, S. Zhang, Periodic propagation of complex-valued hyperbolic-cosine-Gaussian solitons and breathers with complicated light field structure in strongly nonlocal nonlinear media, *Commun. Nonlinear Sci.*, **103** (2021), 106005. <https://doi.org/10.1016/j.cnsns.2021.106005>
30. Z. Y. Sun, D. Deng, Z. G. Pang, Z. J. Yang, Nonlinear transmission dynamics of mutual transformation between array modes and hollow modes in elliptical sine-Gaussian cross-phase beams, *Chaos Soliton. Fract.*, **178** (2024), 114398. <https://doi.org/10.1016/j.chaos.2023.114398>
31. Z. Y. Sun, J. Li, R. Bian, D. Deng, Z. J. Yang, Transmission mode transformation of rotating controllable beams induced by the cross phase, *Opt. Express*, **32** (2024), 9201–9212. <https://doi.org/10.1364/OE.520342>
32. I. M. Batiha, S. A. Njadat, R. M. Batyha, A. Zraiqat, A. Dababneh, Sh. Momani, Design fractional-order PID controllers for single-joint robot arm model, *Int. J. Advance Soft Compu. Appl.*, **14** (2022), 96–114. [10.15849/IJASCA.220720.07](https://doi.org/10.15849/IJASCA.220720.07)
33. H. Qawaqneh, A. Zafar, M. Raheel, A. A. Zaagan, E. H. M. Zahran, A. Cevikel, et al., New soliton solutions of M-fractional Westervelt model in ultrasound imaging via two analytical techniques, *Opt. Quant. Electron.* **56** (2024), 737. <https://doi.org/10.1007/s11082-024-06371-1>

34. A. Zafar, K. K. Ali, M. Raheel, K. S. Nisar, A. Bekir, Abundant M-fractional optical solitons to the perturbed Gerdjikov–Ivanov equation treating the mathematical nonlinear optics, *Opt. Quant. Electron.*, **54** (2022), 25. <https://doi.org/10.1007/s11082-021-03394-w>
35. A. Zafar, A. Bekir, M. Raheel, H. Rezazadeh, Investigation for optical soliton solutions of two nonlinear Schrödinger equations via two concrete finite series methods, *Int. J. Appl. Comput. Math.*, **6** (2020), 65. <https://doi.org/10.1007/s40819-020-00818-1>
36. N. Ullah, M. I. Asjad, J. Awrejcewicz, T. Muhammad, D. Baleanu, On soliton solutions of fractional-order nonlinear model appears in physical sciences, *AIMS Mathematics*, **7** (2022), 7421–7440. <https://doi.org/10.3934/math.2022415>
37. N. Taghizadeh, S. R. M. Noori, S. B. M. Noori, Application of the extended (G'/G) -expansion method to the improved Eckhaus equation, *Appl. Appl. Math.*, **9** (2014), 24.
38. M. Ekici, Soliton and other solutions of nonlinear time fractional parabolic equations using extended (G'/G) -expansion method, *Optik*, **130** (2017), 1312–1319. <https://doi.org/10.1016/j.ijleo.2016.11.104>
39. W. Wu, X. Ma, B. Zeng, H. Zhang, P. Zhang, A novel multivariate grey system model with conformable fractional derivative and its applications, *Comput. Ind. Eng.*, **164** (2022), 107888. <https://doi.org/10.1016/j.cie.2021.107888>
40. R. Khalil, M. A. Horani, A. Yousef, M. Sababheh, A new definition of fractional derivative, *J. Comput. Appl. Math.*, **264** (2014), 65–70. <https://doi.org/10.1016/j.cam.2014.01.002>
41. K. S. Nisar, A. Ciancio, K. K. Ali, M. S. Osman, C. Cattani, D. Baleanu, et al., On beta-time fractional biological population model with abundant solitary wave structures, *Alex. Eng. J.*, **61** (2022), 1996–2008. <https://doi.org/10.1016/j.aej.2021.06.106>
42. N. Al-Salti, E. Karimov, K. Sadarangani, On a differential equation with Caputo-Fabrizio fractional derivative of order $1 \leq \beta \leq 2$ and application to mass-spring-damper system, 2016, arXiv: 1605.07381. <https://doi.org/10.48550/arXiv.1605.07381>
43. A. S. T. Tagne, J. M. E. Ema'a, G. H. Ben-Bolie, D. Buske, A new truncated M-fractional derivative for air pollutant dispersion, *Indian J. Phys.*, **94** (2020), 1777–1784. <https://doi.org/10.1007/s12648-019-01619-z>
44. A. Zafar, A. Bekir, M. Raheel, W. Razzaq, Optical soliton solutions to Biswas-Arshed model with truncated M-fractional derivative, *Optik*, **222** (2020), 165355. <https://doi.org/10.1016/j.ijleo.2020.165355>
45. A. Neirameh, Exact analytical solutions for 3D- Gross-Pitaevskii equation with periodic potential by using the Kudryashov method, *J. Egypt. Math. Soc.*, **24** (2016), 49–53. <https://doi.org/10.1016/j.joems.2014.11.004>
46. M. Ma, Z. Huang, Bright soliton solution of a Gross–Pitaevskii equation, *Appl. Math. Lett.*, **26** (2013), 718–724. <https://doi.org/10.1016/j.aml.2013.02.002>
47. A. A. Bastami, M. R. Belić, D. Milović, N. Z. Petrović, Analytical chirped solutions to the (3+1)-dimensional Gross-Pitaevskii equation for various diffraction and potential functions, *Phys. Rev. E*, **84** (2011), 016606. <https://doi.org/10.1103/PhysRevE.84.016606>

48. T. A. Sulaiman, G. Yel, H. Bulut, M-fractional solitons and periodic wave solutions to the Hirota-Maccari system, *Mod. Phys. Lett. B*, **33** (2019), 1950052. <https://doi.org/10.1142/S0217984919500520>
49. J. V. da C. Sousa, E. C. de Oliveira, A new truncated M -fractional derivative type unifying some fractional derivative types with classical properties, 2017, arXiv: 1704.08187v4. <https://doi.org/10.48550/arXiv.1704.08187>
50. A. T. Ali, E. R. Hassan, General Exp_a -function method for nonlinear evolution equations, *Appl. Math. Comput.*, **217** (2010), 451–459. <https://doi.org/10.1016/j.amc.2010.06.025>
51. E. M. E. Zayed, A. G. Al-Nowehy, Generalized Kudryashov method and general exp_a function method for solving a high order nonlinear schrödinger equation, *J. Space Explor.*, **6** (2017), 120.
52. K. Hosseini, Z. Ayati, R. Ansari, New exact solutions of the Tzitzéica-type equations in non-linear optics using the exp_a function method, *J. Mod. Optic.*, **65** (2018), 847–851. <https://doi.org/10.1080/09500340.2017.1407002>
53. A. Zafar, The exp_a function method and the conformable time-fractional KdV equations, *Nonlinear Eng.*, **8** (2019), 728–732. <https://doi.org/10.1515/nleng-2018-0094>



AIMS Press

© 2024 the Author(s), licensee AIMS Press. This is an open access article distributed under the terms of the Creative Commons Attribution License (<https://creativecommons.org/licenses/by/4.0/>)